Precipitation behaviour of Al–Mg–Si alloys with high silicon content

L. ZHEN, W. D. FEI
P.O. Box 433, Harbin Institute of Technology, Harbin 150001, People's Republic of China
S. B. KANG, H. W. KIM
Korea Institute of Machinery and Meterials, Changwon 641-010, Korea

The precipitation behaviour of three Al–Mg–Si alloys has been studied by differential scanning calorimetry (DSC) and transmission electron microscopy. Seven exothermic peaks are usually observed in DSC thermograms of Al–Mg–Si alloys with high silicon contents. These peaks are believed to be caused by the formation of clusters of silicon and magnesium atoms, Guinier–Preston zones, small precipitates with an unknown structure, β″ phase, B′ phase, silicon precipitates and β phase. The silicon content has no obvious effect on the precipitation of β″ and B′ phases in these alloys, but it has a pronounced influence on the formation of silicon precipitates. The cold-rolling reduction before solution heat treatment is also found to affect the precipitation process appreciably.

1. Introduction

The necessity for a better fuel economy has given rise to an increased number of investigations in the automotive industries. Besides optimizing engine efficiency, the most important effect is obtained by a reduction in body weight. Recent international research and applications by both aluminium and automotive industries seem to concentrate on alloys of the age-hardenable/heat-treatable Al–Mg–Si type [1]. Therefore, more detailed work has been carried out on Al–Mg–Si alloys in recent years [2–5].

Because of the significance in engineering, the precipitation behaviour of Al–Mg–Si alloys have now been studied extensively. However, many details of the precipitation sequence remain the subject of controversy. The following three kinds of precipitation sequences have been proposed: (I) supersaturated solid solution (SSS) → Guinier–Preston (GP) zones → β″ needles → β′ rods → β_{Mg_2Si} plates [6–8]; (II) SSS → clusters of silicon atoms → GP-I zones → GP-II zones/β″ → β′ → β [5]; (III) SSS → independent clusters of magnesium and silicon → co-cluster of magnesium and silicon → small precipitates with unknown structure → β″ needle-shaped precipitates → B′ lath and some β′ rod-shaped precipitates → β [9]. The presence of silicon, in excess of the Al–Mg_2Si pseudo binary composition, is known to enhance the kinetics of the precipitation process without changing the nature of precipitates [8, 10]. Gupta and Lloyd [11] studied a super purity aluminium alloy containing 0.8% Mg and 0.9% Si with differential scanning calorimetry (DSC) and TEM, and suggested that the precipitation sequence is: SSS → clusters and zones → β′ + Si → Si + β → β. But they did not obtain the exothermic peak of silicon precipitation in their DSC thermograms.

Compared to the balanced Al–Mg_2Si alloy, alloys containing an excess silicon are known to have better mechanical properties [1] and therefore important commercial Al–Mg–Si alloys usually contain certain amounts of excess silicon. Even though the precipitation processes in Al–Mg–Si alloys with high excess silicon have been insufficiently studied, these alloys are of great importance both theoretically and in practical use.

In this study, precipitation behaviour and the effects of excess silicon, cold-rolling ratio before solution heat treatment and the time of solution heat treatment on the precipitation behaviour of three Al–Mg–Si alloys with high silicon content were investigated.

2. Experimental procedure

Compositions of the Al–Mg–Si alloys studied here are listed in Table I. The homogenizing treatment of the ingots was carried out by the following process: 430 °C/4 h → 530 °C/20 h then air cooled to room temperature. After hot rolling (a rolling ratio of about 87%) and annealing (400 °C/1 h), the materials were cold rolled to 1, 0.6 and 0.15 mm thick sheets, with the reduction ratios of 67%, 80% and 95%, respectively.

After cold rolling, specimens were solution treated at 550 °C for 2, 30 and 60 min, respectively, and then quenched into water at room temperature. DSC analyses were carried out in a purified argon atmosphere using a Perkin–Elmer DSC7 instrument with a scanning rate of 10 °C min^{-1}. The heat effects associated with the transformation reactions were isolated by subtracting a baseline of a high-purity aluminium–aluminium run. The values of micro-hardness were obtained by using MXT70 digital microhardness tester, with the load of 200 g and holding time of 10 s.

0022–2461

TABLE I Compositions of Al–Mg–Si alloys (wt %)

	Mg	Si	Mn	Zr	Al
A	0.95	0.85	0.3	0.1	Bal.
B	0.95	1.15	0.3	0.1	Bal.
C	0.95	1.55	0.3	0.1	Bal.

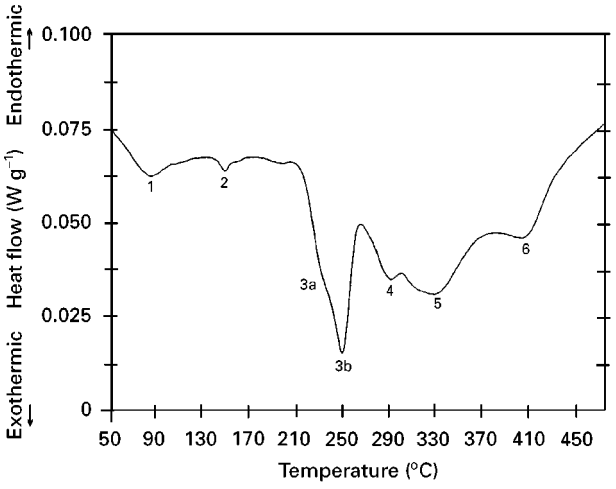

Figure 1 Typical DSC thermogram of alloy C.

For one specimen, each hardness value is the average of seven measurements. Microstructural observation and composition analysis were performed at 160 kV using a Jeol-2000EX type transmission electron microscope equipped with an energy dispersive system (EDS). The specimens for TEM observation were thinned by the standard chemical method.

3. Results and discussion

3.1. Precipitation process of Al–Mg–Si alloys with high silicon content

Fig. 1 shows typical DSC thermograms of alloy C. The specimen was cold rolled with the ratio of 80% before solution heat treatment at 550 °C for 60 min. DSC analysis was performed immediately after solution heat treatment and water quenching. There were six exothermic peaks in the DSC thermogram, which are referred to as peaks 1 to 6. In fact, peak 3 is composed of two peaks, peaks 3a and 3b.

In order to determine the nature of the precipitates at different stages of DSC thermogram, specimens for TEM observation were heated to the peak temperature, T_p, of different exothermic peaks in the DSC instrument using the same conditions as the DSC analyses, held for 3 min and then rapidly cooled down.

TEM observations of specimens heated to the T_p of peak 1 show no obvious contrast. Specimens heated to the T_p of peak 2 were observed using two-beam conditions with $g = \{1\,1\,1\}$, in order to identify GP zones by the strain contrast arising from the lattice misfit. The results are shown in Fig. 2. The contrast observed is very small, which may be attributed to the very small size of GP zones in Al–Mg–Si alloys. Small

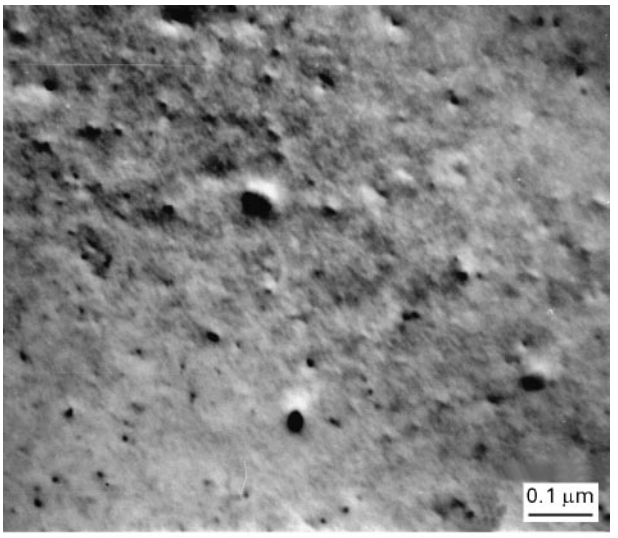

Figure 2 Transmission electron micrograph of alloy C heated to the T_p of peak 2 at 10 °C min^{-1}.

particles are observed at peak 3a, but no obvious diffraction pattern is seen for them, as shown in Fig. 3. Specimens that had been heated to the T_p of peak 3b (250 °C) contain needle-shaped precipitates that are clearly delineated by strain-field contrast (Fig. 4a). Selected-area diffraction patterns (SADPs) taken with $B = [001]_{Al}$ show streaks along $[0\,1\,0]_{Al}$ and $[1\,0\,0]_{Al}$. The appearance of the precipitates, and the SADPs, are in agreement with previous observations for the β″ phase [6]. Lath-shaped precipitates are observed in specimens that had been heated to the T_p of peak 4, and a few large particles are also observed, see Fig. 5a. The lath-shaped precipitates in Al–Mg–Si alloys with an excess silicon are likely to be B′ phase, as reported by Matsuda *et al.* [12]. Large numbers of precipitate particles are present in specimens heated to the T_p of peak 5, and the lath-shaped precipitates have become larger (Fig. 6). Micro-diffraction patterns of the larger particles show that they are silicon precipitates, see Fig. 6b. Fig. 7a shows the transmission electron micrograph of specimens heated to the T_p of peak 6. At this stage, almost all the lath-shaped precipitates are dissolved, only large rods and particles are observed. EDS analyses show that there are both silicon precipitates and β phase (Fig. 7b and c), but it is very difficult to distinguish them from each other on the basis of their morphology.

Edwards *et al.* [9] studied the precipitation behaviour of an Al–0.8Mg–0.79Si alloy by DSC and atom-probe field-ion microscopy (APFIM). They found an exothermic peak in the temperature range of about 30–100 °C, and suggested that it was the result of clustering of independent magnesium and silicon atoms followed by co-clustering of the magnesium and silicon atoms. The shape and position of peak 1 in the DSC thermograms of this investigation are almost the same as that of the study by Edwards *et al.* [9]. Therefore, it is reasonable to suggest that peak 1 is caused by the formation of clusters of magnesium and silicon atoms. The small exothermic peak in temperature range 130–150 °C has not been reported in

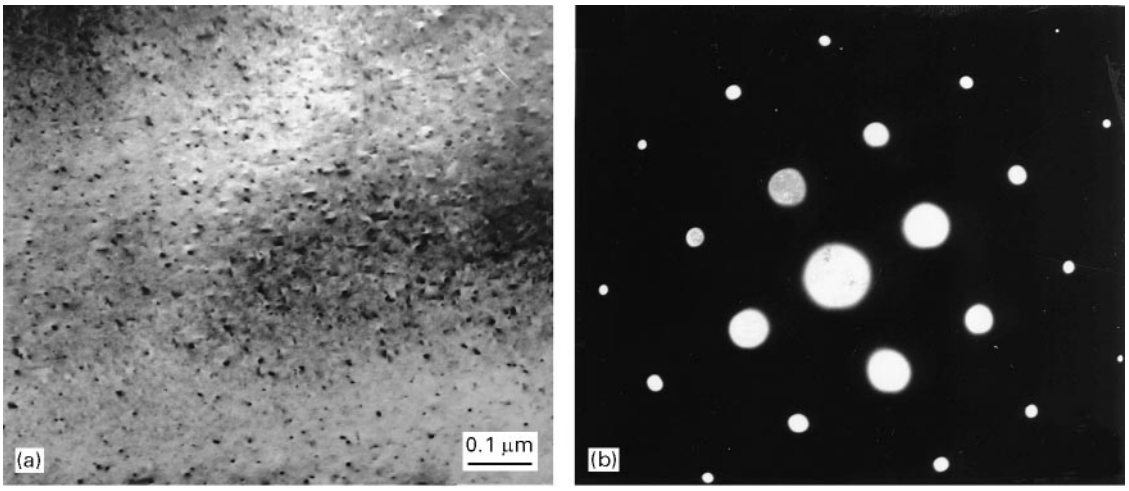

Figure 3 Transmission electron micrographs of alloy C heated to the T_p of peak 3a at 10 °C min^{-1}: (a) bright-field image taken with $B = [0\,0\,1]_{Al}$; (b) diffraction pattern.

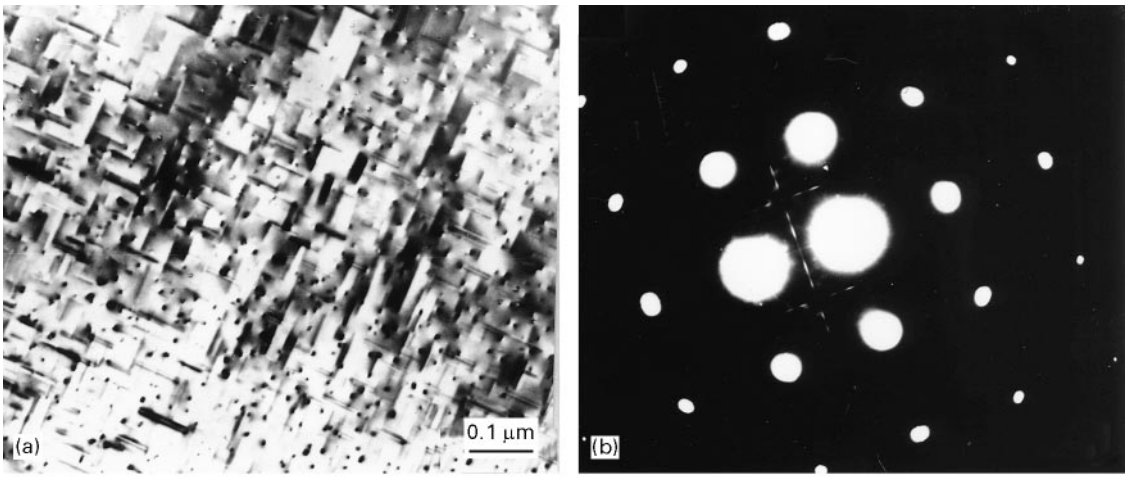

Figure 4 Transmission electron micrographs of alloy C heated to the T_p of peak 3b at 10 °C min^{-1}: (a) bright-field image taken with $B = [0\,0\,1]_{Al}$; (b) diffraction pattern.

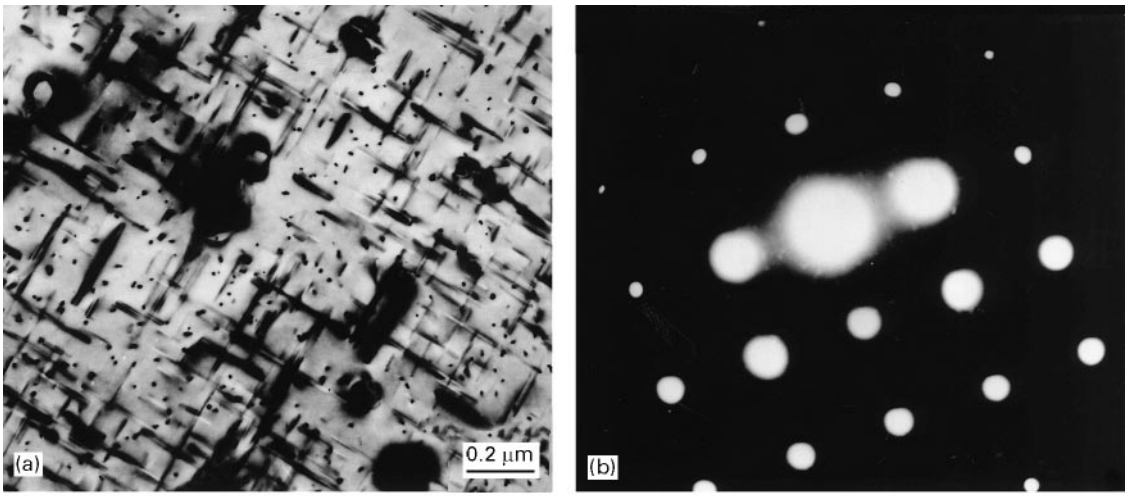

Figure 5 Transmission electron micrographs of alloy C heated to the T_p of peak 4 at 10 °C min^{-1}: (a) bright-field image taken with $B = [0\,0\,1]_{Al}$; (b) diffraction pattern.

previous works. This may be usually caused by the weak calorimetric effect of the exothermic peak. From the contrast observed by TEM of specimens heated to T_p of peak 2 and its position in DSC thermograms, it is suggested that the peak is attributed to the formation of GP zones. The GP zones may be formed directly from part of the clusters formed at lower temperatures. Therefore, the calorimetric effect for the

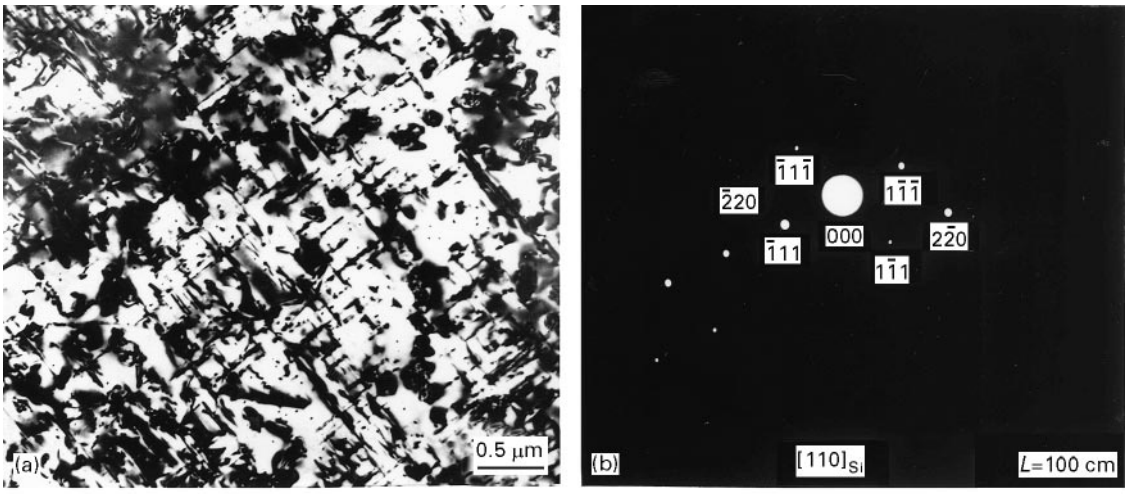

Figure 6 Transmission electron micrographs of alloy C heated to a T_p of peak 5 at 10 °C min^{-1}: (a) bright-field image taken with $B = [0\,0\,1]_{Al}$; (b) micro-diffraction pattern taken from large particles.

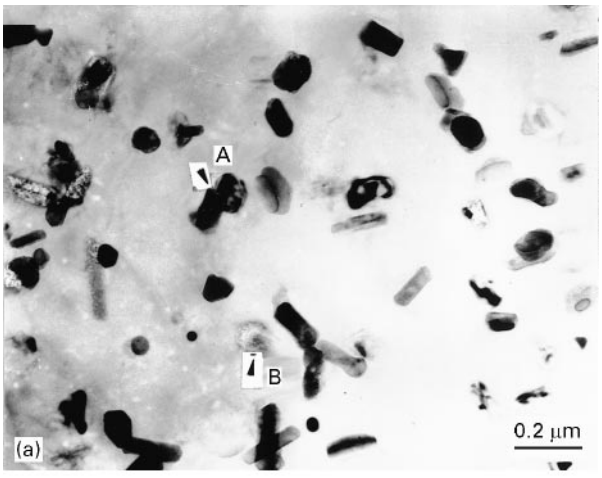

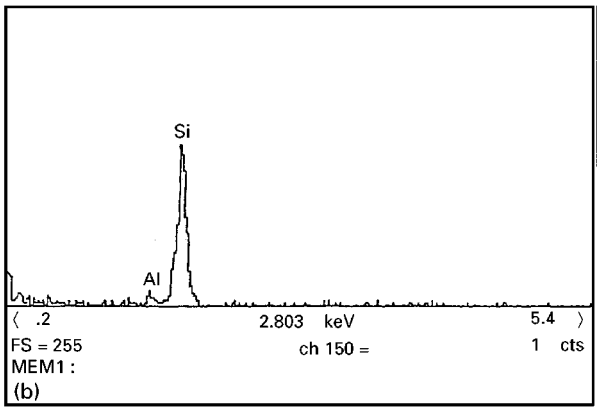

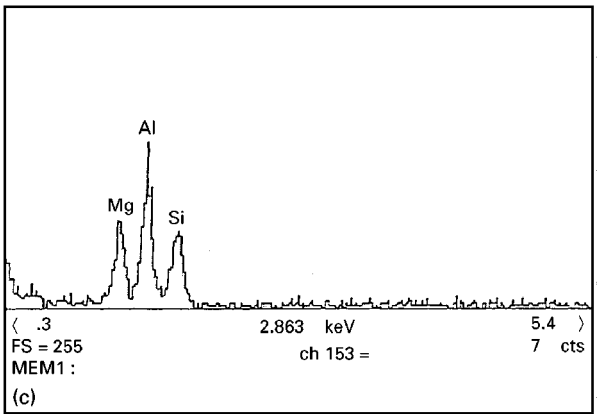

formation of GP zones is small, which may be the reason why peak 2 in DSC thermograms is usually very small. Some small particles are observed at peak 3a by TEM. Edwards *et al.* [9] also found small precipitates in specimens that had been heated to almost the same position of this investigation, but they could not determine their structure even by high-resolution dark-field electron microscopy (HRDEM), so they identified them as small precipitates with unknown structure. They suggested that the main role of this phase in precipitation hardening was to nucleate β″ precipitates. The exothermic peak (peak 3a) caused by the formation of these small precipitates with unknown structure is more pronounced in DSC thermograms of specimens with a high silicon content, or specimens solution heat treated for a long time, inferring that they may be closely related to silicon. Peak 5 is more distinct in DSC thermograms of alloy C, but it has not been reported before. This may be due to the low silicon content in Al–Mg–Si alloys that have been used for the previous investigations. From the experimental results and discussion, the precipitation sequence of Al–Mg–Si alloys with a high silicon content is believed to be:

SSS → independent clusters of Si and Mg atoms, co-clusters of Si and Mg atoms → GP zones → small precipitates with an unknown structure → β″ → B′ → Si precipitates → β.

3.2. Effect of silicon content on precipitation behaviour of Al–Mg–Si alloys

Fig. 8 shows DSC thermograms of specimens prepared from the 1 mm thick sheets of alloys A, B and C in the as-quenched condition. The influence of silicon content on the T_p of exothermic peaks is shown in Fig. 9. It is clearly seen that the silicon content has an obvious influence on the precipitation temperatures of

Figure 7 Transmission electron micrograph of alloy C heated to the T_p of peak 6 at 10 °C min^{-1}: (a) bright-field image; (b) EDS spectra from particle A in (a); (c) EDS spectra from particle B in (a).

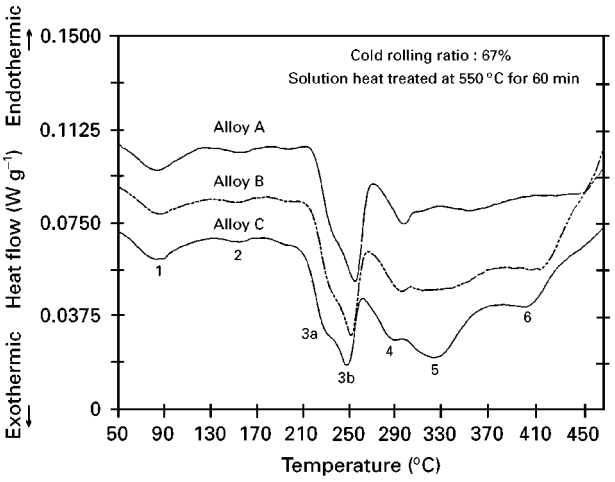

Figure 8 DSC thermograms of specimens prepared from the 1 mm thick sheets of alloys A, B and C in the as-quenched condition.

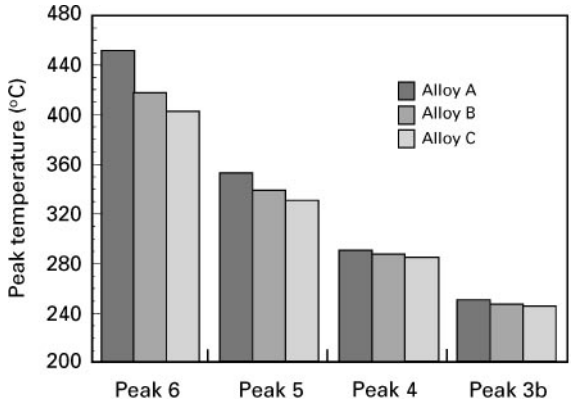

Figure 9 Comparison of T_p of exothermic peaks of alloys A, B and C.

the silicon precipitate and the β phase. The T_p of peak 6 in alloy A is about 50 °C higher than that in alloy C. The influence of silicon content on the T_p of peaks 3b and 4 is small: the T_p of peak 3b in alloy A is only 4 °C higher than that in alloy C. The peak caused by silicon precipitates in alloy C is much more apparent than that in alloys A and B, showing that the volume fraction of silicon precipitates in alloy C is higher than that in either alloy A or alloy B. The peak 3a in DSC thermograms of alloy A is not so apparent as that in alloy C, and it disappears more rapidly with increase in the holding time at room temperature before DSC analysis than that in alloy C. The time between solution heat treatment and DSC analysis has a distinct influence on the precipitation behaviour of Al–Mg–Si alloys, which is discussed in detail in another paper [13]. TEM observations of specimens that have been heated to T_p of different exothermic peaks in DSC thermograms of alloy A are shown in Fig. 10. The major difference between the TEM results of alloy A and alloy C is that almost no silicon precipitates are observed in alloy A at peak 5.

All the three alloys studied in this paper have excess silicon over that required to form stoichiometric Mg_2Si-type precipitates. However, alloy C has a very significant excess of silicon, which leads to the apparent differences in the shape of DSC thermograms between alloy C and the other two alloys. The dominant role of the increased silicon content is to enhance the precipitation of silicon precipitates and β phase. This is caused by the fact that the increase of supersaturation of silicon in the matrix is a very important factor for accelerating the nucleation and growth of precipitates. The minor influence of silicon content on the precipitation of β″ and B′ phases suggests that the precipitation behaviour of the two phases in Al–Mg–Si alloys with high excess silicon is mainly controlled by the magnesium content. Because the peak hardness during artificial ageing is usually connected with the transition of the β″ to B′ phase, it is hence suggested that increasing the silicon content further in Al–Mg–Si alloys with excess silicon does not lead to much improvement in the peak hardness. Therefore, it is not the case that the higher the excess silicon in Al–Mg–Si alloys, the better is the peak strength or hardness after artificial ageing.

3.3. Effect of cold rolling before solution treatment on the precipitation behaviour

As mentioned above, after hot rolling and annealing, the 3 mm thick sheet was cold rolled to 1, 0.6 and 0.15 mm. Specimens were cut from the three different sheets and then solution heat treated at 550 °C for 60 min followed by water quenching. DSC analyses were carried out after these specimens were held at room temperature for 2 h. The results are shown in Fig. 11. It is surprising to see that there are distinct differences among the DSC thermograms of the three kinds of specimens. Firstly the exothermic peak caused by GP zone formation becomes more obvious with an increase in the cold-rolling ratio; secondly there is only one peak in the temperature range 210–250 °C in the DSC thermogram of specimens which experienced the greatest cold-rolling ratio, and the T_p of the peak is much lower; thirdly with an increase of the cold-rolling ratio, the T_p of the exothermic peaks due to silicon precipitates and β phase decreases, see Fig. 12.

TEM specimens prepared from the thinnest sheet were obtained by heating to 230 and 290 °C in the DSC instrument with a heating rate of 10 °C min^{-1} and held for 3 min before being cooled down. The results show that the major precipitate in specimens heated to 230 °C is needle-shaped β″, while many small precipitates with an unknown structure are also observed (indicated by arrows in Fig. 13a). The difference between the small precipitates with an unknown structure and the cross sections of β″ needles is that the former are much larger and usually show a non-circular shape. Such a result shows that peak 3 in the curve of the 95% cold-rolled specimen in Fig. 11 is also composed of two peaks. Two kinds of precipitate are also observed in the specimen that had been heated to 290 °C (Fig. 13b). One is lath-shaped B′ precipitates, and the other is large silicon particles. From the TEM results we can say that, although the

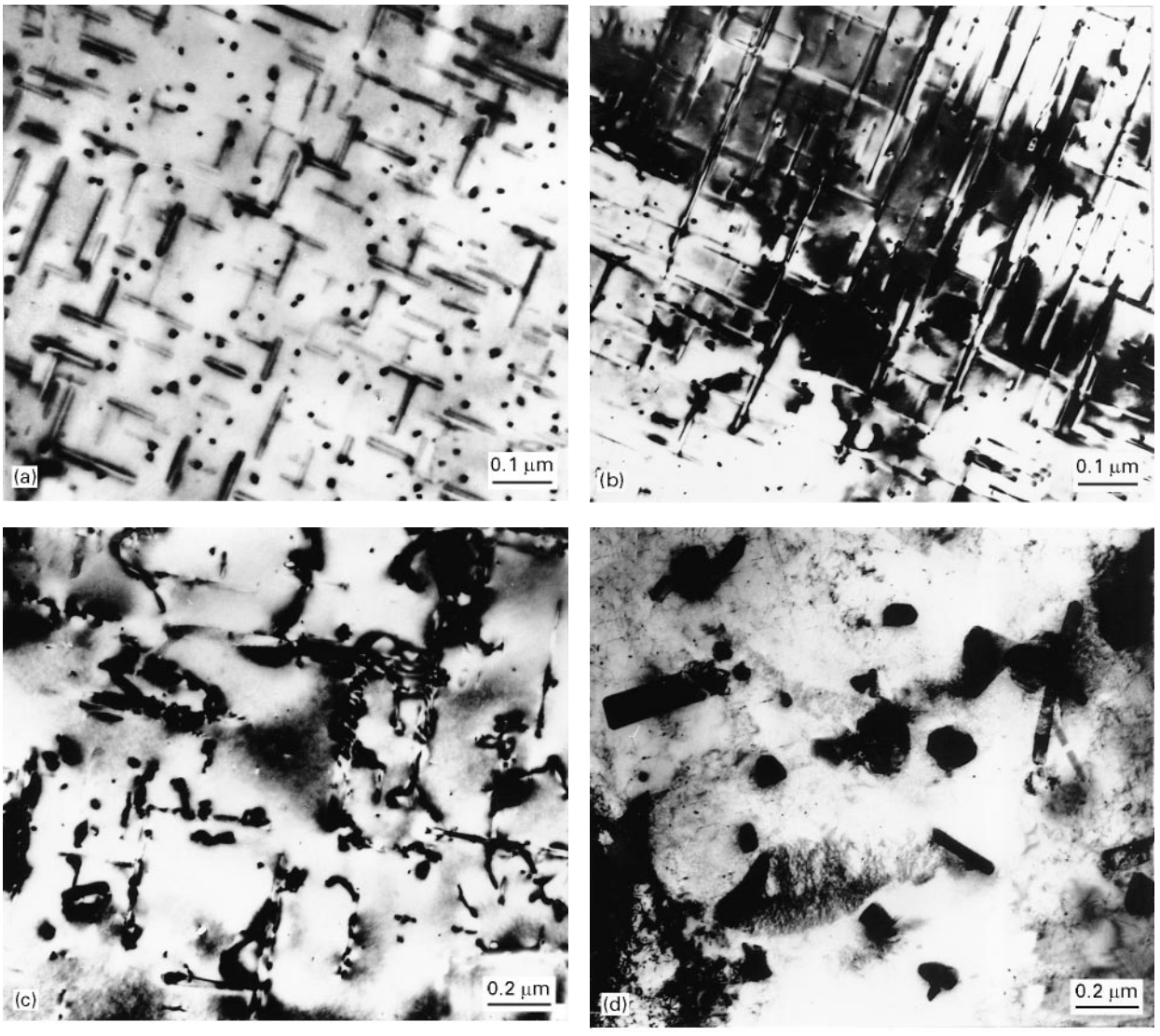

Figure 10 Transmission electron micrographs showing precipitates in specimens heated to the T_p of different exothermic peaks in DSC thermograms of alloy A: (a) at the T_p of peak 3b; (b) at the T_p of peak 4; (c) at the T_p of peak 5; (d) at the T_p of peak 6.

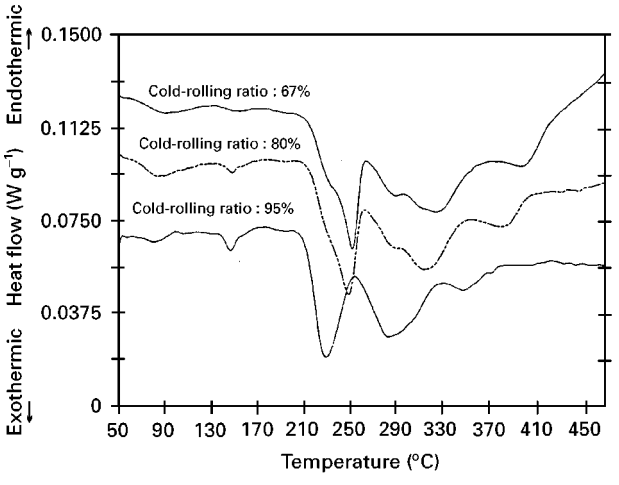

Figure 11 DSC thermograms of alloy C cold rolled with different ratios before solution heat treatment.

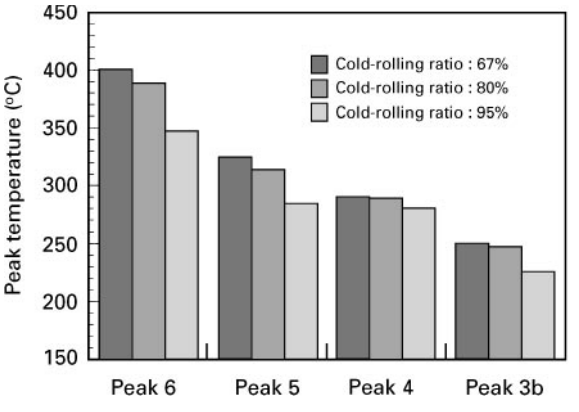

Figure 12 The influence of cold rolling ratio before solution heat treatment on the T_p of exothermic peaks in DSC thermograms of alloy C.

shape of DSC thermogram of the thinnest sheet is different from that of the thicker ones, the precipitation sequence in the three thicknesses of sheet is the same. The increase of cold-rolling ratio only leads to a decrease in the precipitation temperatures of these phases.

With an increase in the cold rolling ratio, the density of defects increases rapidly and they cannot be

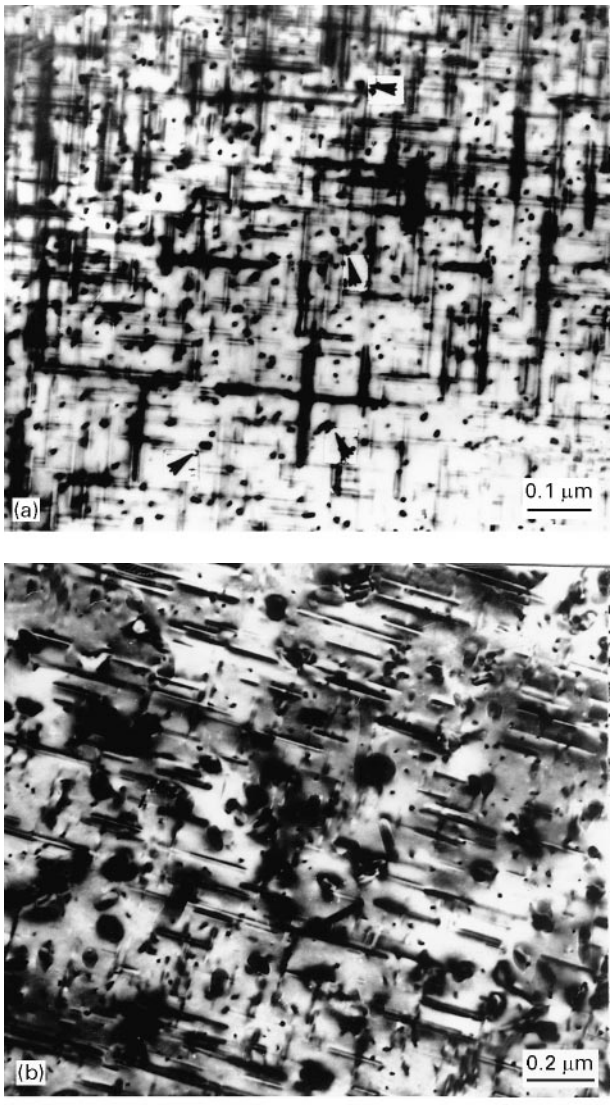

Figure 13 Transmission electron micrographs showing precipitates in specimens of alloy C heated to (a) 230 and (b) 290 °C at 10 °C min^{-1}.

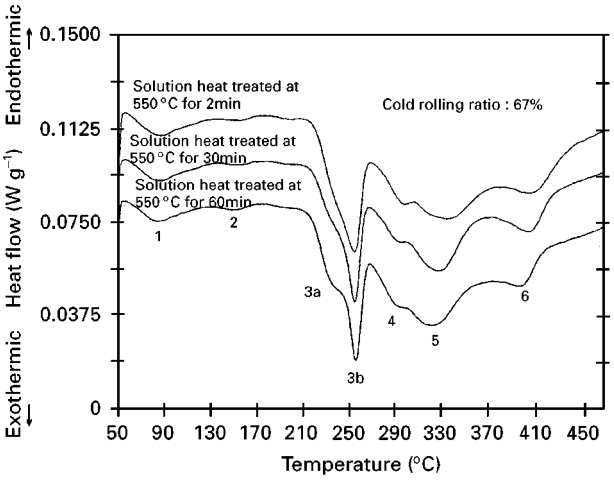

Figure 14 DSC thermograms of alloy C specimens solution heat treated at 550 °C for different times.

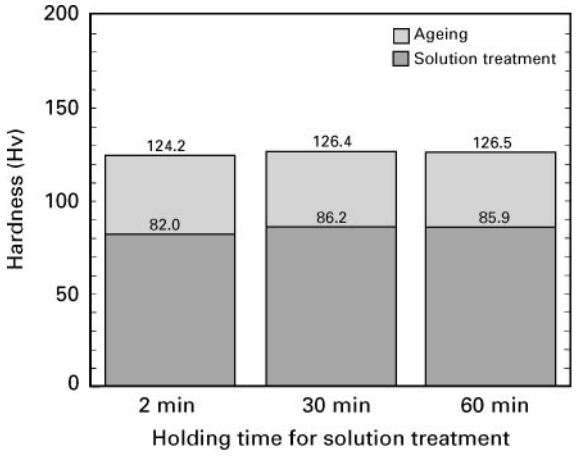

Figure 15 Variation of hardness with holding time for solution treatment in alloy C.

removed completely during solution treatment. This is evinced by the fact that the alloys are not fully recrystallized after solution treatment. Therefore, more defects are retained in the sheet that was cold rolled with the ratio of 95%. The defects can increase the diffusion distance of silicon appreciably, e.g. the diffusion of silicon along dislocations is very rapid and has an activation energy of the order of 0.85 eV as compared with 1.3–1.6 eV in the bulk [14]. Therefore, the precipitation rate in Al–Mg–Si alloys is obviously increased by an increase in the defect concentration, leading to the decrease of T_p of the exothermic peaks. This is possibly also the reason why the exothermic peak of GP zones becomes more obvious with increase of the cold-rolling ratio.

3.4. Effect of the time of solution heat treatment on the precipitation behaviour

Fig. 14 shows the comparison of DSC thermograms of specimens solution heat treated for different times. It clearly shows that peak 3a becomes more obvious with an increase in the time of solution heat treatment, which infers that the more small precipitates with an unknown structure were formed in specimens solution heat treated for long times. Fig. 15 shows the comparison of hardness values of specimens solution heat treated for different times. The hardness values after solution treatment and after ageing treatment of specimens solution heat treated for 2 min are lower than those treated for 30 and 60 min. It is probable that the holding time of 2 min during solution heat treatment is not enough to dissolve the solute into the α-Al matrix completely.

4. Conclusions

1. The precipitation sequence of Al–Mg–Si alloys with high silicon content is believed to be: SSS → independent clusters of silicon and magnesium atoms, co-clusters of silicon and magnesium atoms → GP zones → small precipitates with an unknown structure → β″ → B′ → Si precipitates → β.

2. Adding more excess silicon to Al–Mg–Si alloys that already contain silicon in excess of the pseudobinary Al–Mg_2Si composition does not have a pronounced influence on the precipitation of β″ and B′

phases, but it does promote appreciably the precipitation of silicon precipitates and the small precipitates with an unknown structure.

3. Cold plastic deformation before solution heat treatment has an apparent influence on the precipitation process of Al–Mg–Si alloys. With an increase of the cold rolling ratio, the precipitation temperatures of β″ phase, silicon precipitates and β phase in DSC thermograms obviously decrease. The exothermic peak attributed to the formation of GP zones is more pronounced in the specimens that were cold rolled with the highest ratio.

4. Solute atoms cannot be dissolved completely into the solid solution when Al–Mg–Si alloys are solution heat treated for 2 min.

References

1. G. HUPPERT and E. HORNBOGEN, in "Proceedings of the 4th International Conference on Aluminum Alloys", Atlanta, USA, September 1994, edited by T. H. Sanders Jr and E. A. Starke Jr, Vol. 1 (Georgia Institute of Technology, Atlanta, GA, 1994) p. 628.
2. L. SAGALOWICZ, G. HUG, D. BECHET, P. SAINFORT and G. LAPASSET, *ibid.* p. 636.
3. K. GUGISCH, H. TIMM, W. ULLRICH and F. J. PAEFGEN, *Alumin. Ind.* **12** (1994) 23.
4. W. D. FEI and S. B. KANG, *J. Mater. Sci. Lett.* **14** (1995) 1795.
5. I. DUTTA and S. M. ALLEN, *ibid.* **10** (1991) 323.
6. G. THOMAS, *J. Inst. Metals* **90** (1961–1962) 57.
7. M. H. JACOBS, *Philos. Mag.* **26** (1972) 1.
8. J. P. LYNCH, L. M. BROWN and M. H. JACOBS, *Acta Metall.* **30** (1982) 1389.
9. G. A. EDWARDS, G. L. DUNLOP and M. J. COUPER, in "Proceedings of the 4th International Conference on Aluminum Alloys", Atlanta, Georgia USA, September 1994, edited by T. H. Sanders Jr and E. A. Starke Jr, Vol. 1 (Georgia Institute of Technology, Atlanta, GA, 1994) p. 620.
10. H. WESTENGEN and N. RYUM, *Z. Metallkde* **10** (1979) 528.
11. A. K. GUPTA and D. J. LLOYD, in "Proceedings of the 3rd International Conference on Aluminum Alloys", Trondhiem, Norway: SINTEF, June 1992, edited by L. Arnberg, O. Lohne, E. Ness and N. Ryum, Vol. 2 (Norwegian Institute of Technology, Trondhiem, 1992) , p. 21.
12. K. MATSUDA, Y. UETANI, H. ANADA, S. TADA and S. IKENO, *ibid.* p. 272.
13. L. ZHEN, S. B. KANG and H. W. KIM, *Mater. Sci. Technol.* accepted.
14. G. J. VAN GURP, in "Aluminum alloys: Structure and Properties", edited by L. E. Mondolfo (Butterworths, London, 1976) p. 372.

Received 10 August 1995
and accepted 3 October 1996